An Origin for the Allometric Scaling of Mammalian Fat Reflects Populations Living on the Edge

Justin D. Yeakel,[1,2,*] Mason Fan,[1] Emily Jane McTavish,[1] Anna Carolina de Almeida,[1] Christopher P. Kempes,[2] Luís M. A. Bettencourt,[2,3] Sora Kim,[1] and Greg A. Breed[4]

1. Life and Environmental Sciences, University of California, Merced, California 95343; 2. Santa Fe Institute, Santa Fe, New Mexico 87501; 3. Ecology and Evolution, University of Chicago, Chicago, Illinois 60637; 4. Institute of Arctic Biology, University of Alaska, Fairbanks, Alaska 99775

Submitted October 8, 2025; Accepted May 19, 2026; Electronically published October 12, 2026

Online enhancements: supplemental PDF.

ABSTRACT: Energy stored as adipose fat is the primary endogenous buffer against starvation among mammals, yet fat mass M_f has been understood to scale superlinearly with adult body mass M. Despite the importance of this pattern for hypotheses linking body size to starvation resistance and its potential role in driving the evolution of larger body sizes, its mechanistic origin remains unresolved. Here we combine an expanded empirical synthesis with a minimal mechanistic model to show that superlinear fat scaling is an inevitable consequence of foraging in resource-limited environments. First, assembling seven published datasets—spanning shrews to blue whales—confirms that adding marine mammals and recent terrestrial data produces a new measurement of the mass-fat exponent and leaves the superlinearity unchanged. Second, we explore its origin with a stochastic daily foraging model in which herbivores traverse a bite-scale resource landscape, accruing size-dependent gains and costs. When resources are plentiful and gut limited, gain surplus scales sublinearly, but when resources are scarce and time limited, gain and cost exponents diverge, driving a superlinear gain surplus, which we equate with future fat stores. Matching the empirical exponent requires a 37% daily energetic surplus above maintenance and demographic costs—independent of body size—consistent with populations living near the margin of resource depletion. Together, our framework recasts the mass-fat allometry as a physiological imprint of ecological scarcity rather than purely metabolic design.

Keywords: allometric scaling, fat reserves, foraging energetics, starvation, fasting endurance.

Introduction

Finding enough food to survive and reproduce is a persistent puzzle for most organisms in most environments. Consumed calories must replenish accumulated costs during food acquisition (Hou et al. 2008) in addition to those associated with growth, maintenance, and reproduction (West et al. 2001; Roff 2002). What remains represents an energetic surplus, which can be saved in different storage tissues, depending on species, to be used at a later date when food is less available. Whereas birds and fish store surplus energy as lipids—in birds, within subcutaneous fat pads and the liver, and in fish, within the liver, myosepta, and buoyant lipid deposits like those in some swim bladders (Weil et al. 2013)—mammals primarily store energetic reserves in adipocyte cells that form adipose tissue (Pond 1992). Among caching species (e.g., some birds and mammals, including humans), these stores can be coupled with exogenous reserves, though the latter must be deposited and left behind (Brodin 2010; Kelt 2011; Yeakel et al. 2020). For most species, endogenous stores alone represent an individual's entire energetic buffer against hard times.

Among mammals, larger species tend to have near-isometric amounts of muscle, guts, and bone (Lindstedt and Calder 1981). As such, these volumetric tissues roughly scale $\propto M^{1.0}$, where M (kg) is adult body mass. Famously, mammalian fat mass $M_f = f_0 M^{f_1}$ (kg) does not follow this expectation and instead scales superlinearly, where the most commonly accepted exponent ($\pm$SE) is $f_1 \approx 1.19 \pm 0.025$ (Lindstedt and Boyce 1985). This superlinear mass-fat scaling means that larger species tend to carry a greater proportion of their body weight as fat. It is this relationship that serves as the fulcrum for the fasting endurance hypothesis (Millar and Hickling 1990), which describes an evolutionary advantage of larger body size arising from greater starvation resistance. Inclusion of superlinear mass-fat scaling into models of starvation dynamics has resulted in accurate theoretical predictions of the largest terrestrial mammal body size (Yeakel et al.

* Corresponding author; email: jyeakel@ucmerced.edu.

American Naturalist, volume 208, number 5, November 2026. © 2026 The University of Chicago. All rights reserved, including rights for text and data mining and training of artificial intelligence technologies or similar technologies. Published by The University of Chicago Press for The American Society of Naturalists. https://doi.org/10.1086/742753

2018), the evolutionary advantages of grazing (Bhat et al. 2020), and megaherbivore extinction risk (Rallings et al. 2024). Although the superlinear mass-fat relationship clearly has important consequences for selection and long-term macroevolutionary trends, its origin has not been explored.

Here we reexamine the mass-fat relationship, assembling seven published datasets to quantify the allometry of fat. We then propose a theoretical framework for the origin of the mass-fat relationship based on the intersection of daily foraging mechanics and resource scarcity in different types of environments. The physiological incorporation and synthesis of fat has received much attention; however, the role that acquisition plays in governing the energetic surplus that is later routed to fat is less well understood. Because the amount of fat carried by an organism reflects the limits of acquisition and maintenance before hitting physiological or mechanical bounds, we suggest that this perspective is necessary to understand the superlinear scaling of body fat observed in nature.

Methods and Model Description

Empirical Analysis

Mammalian fat and body mass data were compiled from a number of previously published sources, which have heretofore not been assessed as a whole. The foundational mass-fat relationship was derived from species averages collected by Pitts and Bullard (1968), expanded upon by Pond and Mattacks (1985), and reevaluated by Calder (1996) and later Lindstedt and Schaeffer (2002). In addition to data from these sources, we also include a large dataset from Navarrete et al. (2011) primarily composed of smaller-bodied rodents, primates, and carnivores from both wild and captive environments.

To address the lack of representation of marine mammals, we included measurements of pinnipeds and mysticetes from Ryg et al. (1993) in addition to several individual bowhead whales (George et al. 2007), where a relationship was established between body fat and the number of barrels harvested by commercial whalers. Using this barrel-to-fat conversion, we included estimates for sperm whales, right whales, and pilot whales, among others, based on reports from the American Offshore Whaling Logbook spanning 1784–1920 (Lund et al. 2025). These combined datasets cover 57 families and span seven orders of magnitude in body size represented by mammals in both terrestrial and aquatic environments as well as a handful of aerial bat species (see app. S1; apps. S1–S5 are available online).

Foraging Model

We explored a potential origin for the superlinear mass-fat scaling premised on daily foraging dynamics. This framework is premised and parameterized for larger-bodied terrestrial herbivores (e.g., small gazelles to megaherbivores) surface foraging within a resource volume, such as a closed canopy forest or woodland where resources are distributed both horizontally and vertically. Direct extensions to address constraints imposed by alternative environments, such as aquatic systems or even for organisms functioning at different trophic levels, will require minimal alterations, which we expand upon in "Results and Discussion."

Our minimal foraging model predicts the daily energetic gain g (kJ day^{-1}) and costs c (kJ day^{-1}) of an individual mammalian forager with body mass M as it accumulates food within a daily foraging bout (table 1). Throughout the foraging bout, we accounted for accumulated daily gains and costs differently, depending on whether the herbivore fills its gut or reaches the end of the bout with its gut partially full. If the forager's gut is filled, gains are equivalent to its gut capacity. If the forager's gut is not filled, gains are proportional to the number of resource encounters it has within the bout. Energetic costs c (kJ day^{-1}) are similarly accrued with respect to the different actions (travel, chewing, and rest) taken during and outside the foraging bout. We assume that the energetic cost accrued during travel scales with the forager's field metabolic rate, whereas that accrued while chewing and postbout scale with the forager's basal metabolic rate, both of which $\propto M^{0.75}$ (Nagy 2005). We next describe how encounters with resources

Table 1: Model parameters, definitions, and units

Parameter	Definition	Units
μ	Resource volumetric density	g · m^{-3}
α	Resource dispersion	. . .
ζ	Resource patchiness exponent	. . .
δ	Resource energy density	kJ · g^{-1}
M	Forager body mass	kg
$M_f = f_0 M^{f_1}$	Forager fat mass	kg
β	Forager bite size	g · bite^{-1}
v	Forager velocity	m · s^{-1}
$q = \mu/\beta$	Landscape bite density	bites · m^{-3}
n	Competitive load	individuals · m^{-2}
D	Distance between bites	m
g	Forager daily energetic gains	kJ · day^{-1}
c	Forager daily energetic costs	kJ · day^{-1}
γ	Mass-fat scaling exponent	. . .
$\phi = g/c$	Reserve ratio	. . .

Note: For details, see appendix S2.

account for the gains a forager achieves within a bout in environments with different patchiness effects, followed by a description of the temporal constraints determining the time allotted to each resource encounter and daily foraging bouts as a whole.

Resource encounters. The forager encounters resources drawn from a spatial resource distribution normalized to the size of the forager's bite, which we refer to as the bite density field (bites m^{-3}). The spatially implicit distribution of resources is defined by the raw volumetric resource density μ (g m^{-3}) and resource dispersion α (unitless), which captures spatial resource variability. A herbivore's resource encounters within that vegetative volume are then scaled to the organism's bite size β (g $bite^{-1}$), which itself varies with body mass and is roughly volumetric (i.e., near-isometric with body volume), where $\beta \propto M^{0.96}$ (Shipley et al. 1994). Because one bite contains β grams of plant tissue, bite density is $q = \mu/\beta$. Thus, as body mass increases and β grows, a fixed resource density translates into a lower bite density, reflecting the coarser sampling of larger herbivores. Herbivores thus travel from bite to bite with velocity $v \propto M^{0.13}$ (m s^{-1}) (where speed increases sublinearly with body size via limb length scaling; Kramer and Prins 2010) across an implicit bite density field.

We assume that the focal herbivore must share the resources contained in its instantaneous reaction cross section, a body size–dependent plane of width w and height h (purple and blue panes in fig. 1), with a local competitor load $n = d/(wh)$ (individuals m^{-2}), where d is the number of conspecifics expected to share the daily foraging corridor (along purple and blue trailing lines in fig. 1), which, with the animal's reaction cross section sweeping through, defines the sampling volume (Carbone et al. 2014). Because competitors follow broadly parallel daylong foraging trajectories, we treat their effect as a continuous competitive load acting uniformly across the focal animal's reaction cross section during the bout, thus including a static competitive limitation on resource availability.

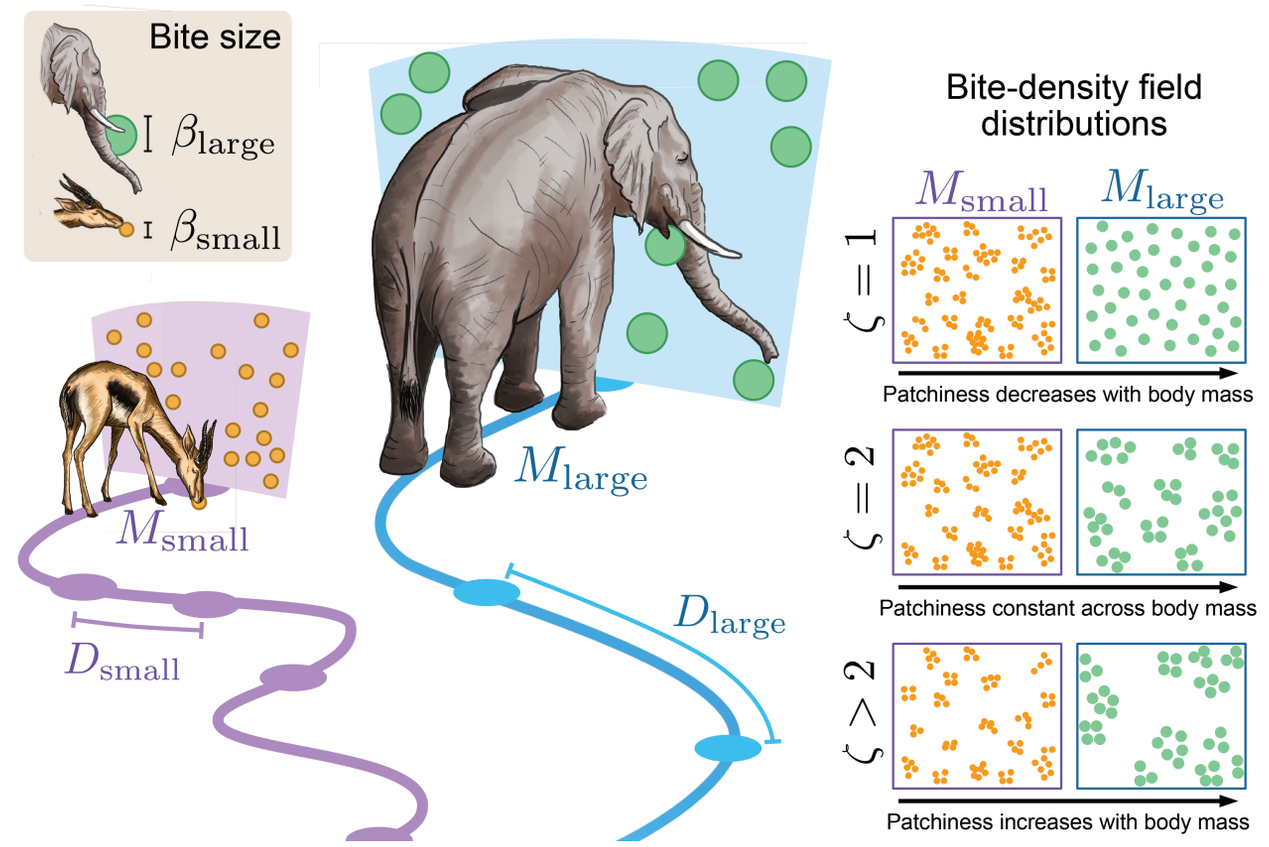


Figure 1: Schematic of foraging process, where foraging herbivores of different masses travel D meters from bite to bite as function of their reaction cross section (purple and blue planes) and where bite size (β; orange and green circles) scales with mass (top left inset). The bite density field distribution defines the mean, dispersion, and patchiness scaling of bites, respectively, across an implicit landscape. Right inset panels show top-down views of the bite density landscape as a function of forager size M and patchiness exponent ζ. When $\zeta = 1$, patchiness decreases with forager mass M; when $\zeta = 2$, patchiness is constant across M; when $\zeta > 2$, patchiness increases with M.

The spatial patchiness of resources changes as a function of organismal body size. For example, a habitat with evenly distributed foods may look heterogeneous to a small forager but homogeneous to a large forager (Bhat et al. 2020). On the other hand, foods that are very patchy, such as some fruits, may be expected to retain their patchiness with increasing body size. In some systems, the patchiness of resource distributions may be expected to increase with consumer size; for example, megaherbivores such as elephants engineer nutrient-rich grazing islands in miombo woodlands, intensifying clumping at the spatial scales experienced by large foragers (Kohi et al. 2011; Kartzinel et al. 2014; Coverdale et al. 2016). The interaction between the mean and variability of encounters between a consumer and its resources largely determines the gain required to replenish daily costs and whether a forager will be in a state of energetic surplus or deficit by the end of a foraging bout.

Following spatial-partitioning frameworks (e.g., Holland et al. 2009; Bhat et al. 2020), the mean and variance of bite encounters experienced by an individual is rescaled by competitive load as $q_{\text{ind}} = q/n$ and $\sigma^2_{\text{ind}} = q^2/(n^\zeta \alpha)$ (such that $\alpha_{\text{ind}} = \alpha n^{\zeta-2}$), respectively, where the exponent ζ modulates how much patchiness persists after resources are subdivided among conspecifics (see inset of fig. 1). The scaling of patchiness and size is thus determined by the exponent ζ, and its effect on the scaling of the resource distribution with body size can be observed with the coefficient of variation (CV), expressed as

$$\text{CV}_{\text{res}} = \frac{n^{1-\zeta/2}}{\sqrt{\alpha}}. \tag{1}$$

From equation (1), we observe that when $\zeta = 1$, resource distributions become more homogenous as the herbivore increases in size (i.e., CV_{res} declines with mass; see inset of fig. 1), whereas when $\zeta = 2$, resource distributions retain their inherent patchiness (i.e., CV_{res} is constant with mass). We also investigated a scenario where $\zeta > 2$ such that patchiness increases with consumer size (i.e., CV_{res} increases with mass; app. S2).

For a homogeneous resource field, the distance between successive bites D is constant for a given body mass. (Throughout, stochastic quantities are represented by uppercase notation, whereas particular values of stochastic quantities are denoted by lowercase notation.) This interbite distance increases with body mass, as the bite density field grows more coarsely divided with increasing forager size. To capture spatial heterogeneity, we invoke a maximum entropy argument and assume that the bite encounter rate follows a gamma distribution, where $\Lambda \sim \text{gamma}(\alpha_{\text{ind}}, q_{\text{ind}}/\alpha_{\text{ind}})$, so that $\mathbb{E}\{\Lambda\} = q_{\text{ind}}$ and $\text{var}\{\Lambda\} = q^2_{\text{ind}}/\alpha_{\text{ind}}$. We thus encode the minimum set of constraints on this distribution, including restricting Λ to positive values and constraining only its mean and dispersion; other distributions with similar constraints are not expected to alter model results. Conditional on Λ, the distance between resources is drawn from $D|\Lambda \sim \text{exponential}(\text{rate} = \Lambda)$. This gamma-exponential mixture (a Lomax/Pareto type II distribution) captures the heavy-tailed spacing that arises when food patches are highly clumped. As the forager moves forward through its environment bite by bite, it samples a vertical cross section of resources sweeping through a three-dimensional volume (fig. 1). The expected distance between bites along the forager's path (m) can then be expressed as

$$\mathbb{E}\{D = d\} = \frac{\alpha n^{\zeta-1}}{q(\alpha n^{\zeta-2} - 1)}. \tag{2}$$

Temporal constraints. Bites of resources accumulate as the forager travels, with the expected travel time between each bite given by $t_{\text{t}} = \mathbb{E}\{D\}v^{-1}$, where v is the forager's velocity. With each encounter, the forager pauses to chew its bite, where the time to chew is given by $t_{\text{c}} \propto M^{0.196}$ (Žliobaitė and Fortelius 2018). The travel, encounter-bite-chew, travel sequence continues until one of two end points: the forager either fills its gut or reaches the end of its foraging bout. The temporal length of the forager's bout is assumed to follow the scaling relationship observed for terrestrial megaherbivores, where $t_{\text{b}} \propto M^{0.124}$ (Owen-Smith 1988). Thus, larger herbivores tend to spend more absolute time chewing and foraging, even as mass-specific energetic requirements decline with body size. While the t_{b} allometry is largely phenomenological, we note that alterations to this exponent do not strongly impact the nature of our results (app. S2). Here we assume that each foraging bout is independent such that we do not examine coupled dynamics across multiple days, nor do we include the dynamics of gut passage and the potential for multiple foraging bouts within a day. Because gut retention time is typically longer than the expected bout length, particularly for larger-bodied herbivores, we make the simplifying assumption that a full stomach marks the end of the bout if the forager is able to fill it.

Herbivore gut capacity scales differently with body mass, depending on the type of fermentation employed. We examine four different modes of herbivory with different gut capacity scalings: cecum fermenters (gut capacity $u_{\text{ca}} \propto M^{0.86}$), colon fermenters ($u_{\text{co}} \propto M^{0.92}$), nonrumen foregut fermenters ($u_{\text{nrf}} \propto M^{0.88}$), and rumen foregut fermenters ($u_{\text{rf}} \propto M^{0.90}$), where gut capacity is measured in grams of dry mass (Müller et al. 2013). Across these four fermentation modes, the fitted gut capacity relationships span a large range, corresponding to an envelope $u_{\text{max}}/u_{\text{min}} = 1.64 \times M^{0.037}$ (~2.1-fold at $M = 900$ kg).

Throughout, we converted gut capacity to kilojoules assuming an energy density similar to that of grass, $\delta = 18.2$ (kJ g^{-1}).

See appendix S2 for details on all included allometric relationships. We note that although we do not include the observed negative relationship between resource quality and biomass density (Fryxell 1991; Bergman et al. 2001), we demonstrate in appendix S2.D that its inclusion does not alter our results.

Results and Discussion

The superlinearity of the mammalian mass-fat scaling relationship has long been recognized for its impact on the fitness advantages associated with larger body sizes, though its origin is unknown. We first present a reevaluation of the empirical mass-fat relationship, combining seven previously published datasets, where we assessed whether and to what extent it is sensitive to phylogenetic relatedness, dataset-specific biases, and/or differences between the foraging modes associated with included mammalian species. Second, we describe the allometry of predicted daily foraging gains and costs as a function of herbivore body size under both resource-plentiful and resource-limited environments and discuss under what conditions the gain surplus (which we argue is proportional to fat reserves) is expected to be superlinear. Third, we show that the observed mass-fat scaling suggests that mammalian populations are balanced near the edge of resource limitation, and we evaluate the maximal energetic surplus required to give rise to the observed scaling relationship. Finally, we discuss extensions and applications of our framework to different foraging environments and types of foragers, including mysticete whales.

Reassessing the Empirical Mass-Fat Scaling

Integrating across datasets (number of species observations, $n_{\text{obs}} = 218$; fig. 2), we found that standard ordinary least squares (OLS) regression gives a superlinear mass-fat exponent of $f_1^{\text{OLS}} = 1.134 \pm 0.015$ (SE; $t = 75.94$, $P \ll .001$). Cetacean species with fat mass extrapolated from the barrel-to-fat conversion were excluded. To examine whether phylogenetic relationships altered the observed scaling, we repeated the analysis on the subset of records for which genus- and species-level identifications were available utilizing the Open Tree of Life R package rotl.R (Michonneau et al. 2016). We fitted both the OLS model and a phylogenetic generalized least squares (PGLS) model under a Brownian motion error structure (i.e., Pagel's λ

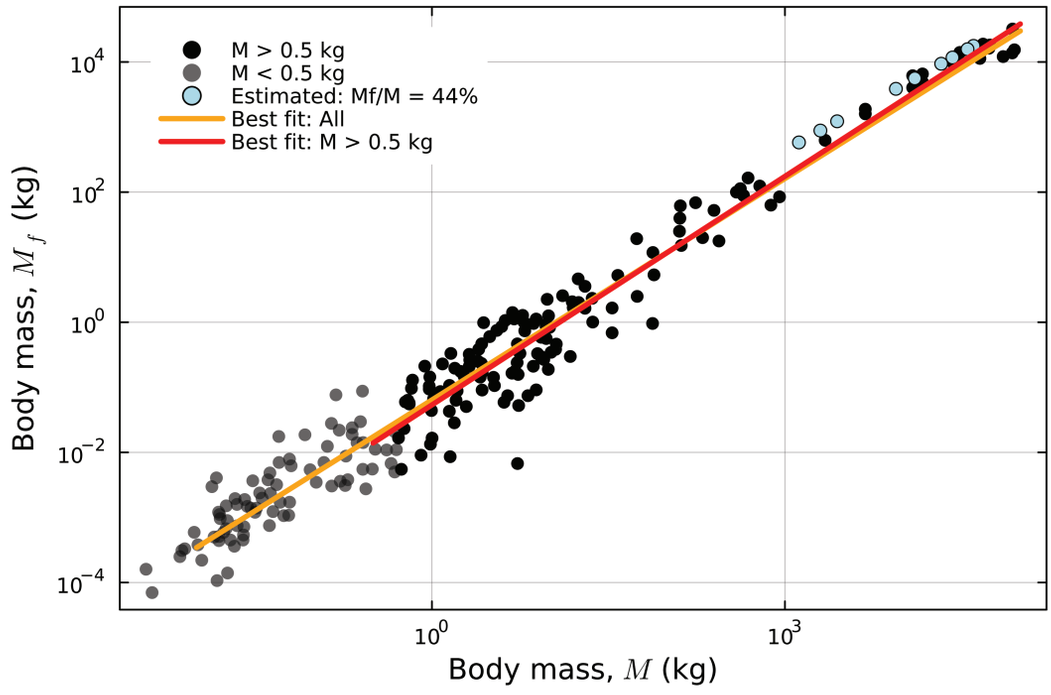


Figure 2: Empirical mass-fat relationship using OLS. Best fit for the full dataset has a slope of 1.134 ± 0.015 (SE; red line). The OLS best fit for species with $M > 0.5$ kg is 1.171 ± 0.023 (SE; orange line); the PGLS best fit for larger species is 1.139 ± 0.061 (not shown for clarity).

fixed at 1 rather than estimated) on a pruned tree containing 158 tips and 848 internal nodes, scaled to time with branch lengths in units of millions of years (McTavish 2025). For this matched subset, the PGLS fit yielded $f_1^{\mathrm{PGLS}} = 1.145 \pm 0.052$. The PGLS 95% confidence interval encompasses the OLS estimate, so the phylogenetic correction did not materially change the exponent (app. S1). Overall, accounting for shared evolutionary history did not change the conclusion that mammalian fat mass scales superlinearly with body mass.

To check whether this estimate is distorted by idiosyncratic differences among studies, we fitted linear mixed effects models with each of the seven datasets as a grouping factor. A random intercept model of the full set of measures (using OLS) allows each dataset its own vertical offset and yielded an exponent of $f_1^{\mathrm{OLS}} = 1.118 \pm 0.017$; the between-dataset SD of those offsets was 0.20 log units (approximately $\pm 22\%$), whereas within-dataset scatter remained much larger (residual SD = 0.91). Adding dataset-specific slopes did not improve fit ($\chi^2_2 = 2.91$, $P = .23$; $\Delta\mathrm{BIC} = 7.86$), so the simpler random intercept model was retained. Likewise, a fixed effects ANCOVA that includes a full set of dataset-specific intercepts and slopes reduced residual variance ($F_{10,205} = 3.07$, $P = .001$) but left the common slope within the mixed model 95% confidence limits. Together, these analyses confirm that the exponent of approximately $f_1^{\mathrm{OLS}} = 1.13$ was robust to model specification and study-level variation.

Because the combined dataset spans terrestrial, aquatic, and aerial mammals—foraging modes that confront markedly different energetic regimes and mechanical constraints—we next tested whether habitat categorizations altered the mass-fat scaling relationship. A mixed effects model allowing mode-specific intercepts gave a virtually identical slope ($f_1^{\mathrm{OLS}} = 1.122 \pm 0.018$). Although adding mode-specific slopes changed the log likelihood by less than 0.03 units ($\chi^2_2 = 0.05$, $P = .97$), the model was disfavored by information criteria ($\Delta\mathrm{BIC} = 10.7$), so we retained the pooled line. Translating the coefficients into mode-specific exponents using fixed effects ANCOVA yielded $f_1^{\mathrm{OLS,aer}} = 1.37 \pm 0.30$ for aerial species, $f_1^{\mathrm{OLS,aq}} = 1.15 \pm 0.04$ for aquatic species, and $f_1^{\mathrm{OLS,terr}} = 1.11 \pm 0.02$ for terrestrial species. Pairwise Wald tests showed that neither the aerial-terrestrial difference ($t = 0.89$, $P = .37$) nor the aerial-aquatic difference ($t = 0.74$, $P = .46$) was individually significant and that aquatic and terrestrial slopes were statistically indistinguishable. It is possible that the notably steeper slope for aerial species may represent a true biological signal, but this will require a more rigorous investigation given that our dataset is limited to 14 chiropteran species. We theorize that a steeper mass-fat relationship for aerial species might be driven by the increased energetic demands of flight, particularly for larger species (Voigt et al. 2010). In contrast, similar mass-fat scaling relationships for terrestrial and aquatic species is in line with our primary hypothesis: that an organism's fat is driven primarily by limitations associated with foraging, even if gravitational constraints are relaxed, as is the case for aquatic foragers.

Our theoretical model is primarily focused on mammalian species acquiring food sequentially and stepwise on the surface landscape. When we excluded the smallest species ($M < 0.5$ kg), which are dominated by bats and burrowing or caching rodents, whose foraging dynamics diverge from our model assumptions, we observed a steeper mass-fat relationship for the OLS fit, while the PGLS fit remained effectively the same. An ANCOVA contrasting the small-bodied taxa ($M \leq 0.5$ kg) against the large-bodied subset ($M > 0.5$ kg) indicated that small species followed a shallower scaling of $f_1^{\mathrm{OLS,small}} = 1.01 \pm 0.08$. This slope was 0.16 ± 0.09 lower than that of the large-bodied class, a difference that approaches but does not reach significance ($t_{214} = -1.88$, $P = .061$). Size class had no detectable effect on intercepts ($P = .71$).

After removing the small-bodied species, the remaining taxa yielded an internally consistent exponent of $f_1^{\mathrm{OLS}} = 1.171 \pm 0.023$, effectively reproducing the previously observed 1.19 value (Pitts and Bullard 1968; Lindstedt and Boyce 1985; Lindstedt and Schaeffer 2002), which comfortably overlapped the mass-fat slope estimate of $f_1^{\mathrm{PGLS}} = 1.14 \pm 0.06$ using PGLS. Throughout, we report both the conventional OLS slope (for direct comparability with the historical literature and our 138-species dataset) and the phylogenetically corrected PGLS slope (to account for nonindependence among related taxa), using these measures to bracket subsequent analyses (see app. S1 for additional details).

An Origin for the Mass-Fat Scaling Relationship from Foraging Dynamics

Mammalian bones, muscles, guts, and integument are all structural and organ systems that have well-defined and largely isometric scalings across species of different body sizes (Lindstedt and Schaeffer 2002). It is clear that fat does not follow the isometry typical of other volumetric anatomies and can vary dramatically depending on the prevailing environmental conditions, life history of the organism, and, in particular, whether a species is aquatic or terrestrial (Lindstedt and Boyce 1985; Millar and Hickling 1990). It is tempting to think of adipose fat as a tissue that fills an implicit and bounded compartment, and although there are certain biophysical boundaries where an organism would have so much fat that it could no longer function, such boundaries are rarely observed in nature. Instead, the observed limits of body fat

for mammalian individuals tend to be far from states observed in resource-replete environments, such as in captivity, where health complications from fat accumulation are common (Schook et al. 2015; Chusyd et al. 2021). If the amount of fat that individuals carry is instead limited by the environment, it stands to reason that the observed superlinear mass-fat scaling may arise from the intersection of resource limitation and the mechanics of foraging.

To examine this intersection, we used our minimal foraging model, which captures the daily energetics of herbivores of different sizes traveling across a resource landscape. We evaluated the accumulated daily gains g and costs c (kJ day^{-1}) across 1,000 independent realizations for every environmental and body size combination, which we confirmed to be more than enough to achieve stationarity in our results.

Anabolism of endogenous fat stores requires that the foraging organism has, on average, gains that surpass costs, which we formalize as the gain surplus, $g_S = g - c$. If foraged gain is only enough to replenish daily costs ($g = c$), there is no excess from which to synthesize fat. We might therefore surmise that the degree to which there is surplus determines directly the degree to which an organism can add to its endogenous fat stores. If the proportion of ingesta assimilated into the body (η) remains constant across body mass, g_S can be assumed to have the same scaling as the mass-fat relationship. Digestive efficiency, or the proportion of ingesta retained in the body, best approximates this notion of η and has been shown to be roughly constant across herbivore body mass, ranging from $\eta = 0.45$–0.65, but with no clear allometric signal (Clauss and Hummel 2005). Müller et al. (2013) similarly found little evidence that digestive efficiency increases with body size, suggesting that larger herbivores instead compensate for lower-quality forage primarily by increasing intake.

Fat stores are accumulated over time from the gain surplus, and it is the allometry of this integrated tissue that is captured in the mass-fat relationship. We show in appendix S3 that under most conditions where energetic reserves are accumulated over seasonal periods of gain followed by loss, fat storage is expected to have the same exponent as the daily gain surplus. Given this approximate equivalence, throughout we use the exponent of the gain surplus term to relate directly to the scaling of fat tissue among mammals. We next investigate whether g_S scales with mass superlinearly such that $g_S \propto M^{\gamma>1}$ and under what conditions it may be expected to approach the observed mass-fat scaling, where $\gamma \approx f_1$.

Gut capacity constrains gains in rich environments. When resources are plentiful, individual foragers are able to fill their gut prior to the end of a foraging bout. In such environments, the travel time between bites is short, allowing individuals to achieve high rates of gain at lower expense. In this case, we expect $g \approx \delta g^{\text{gut}}$, where g^{gut} is the herbivore's gut capacity (g) such that $g^{\text{gut}} = g_0^{\text{gut}} M^{g_1^{\text{gut}}}$, with different exponents for different fermentation pathways.

We calculated the gain surplus exponent γ, where $g_S \propto M^{\gamma}$, from daily simulations of foragers with body masses ranging from $M = 50$ to $M = 25{,}000$ kg, roughly the size of a small gazelle to 1.5× the size estimates for the largest terrestrial mammalian herbivores, which include *Paraceratherium* and *Deinotherium* (Yeakel et al. 2018). For each value of environmental richness μ and patchiness ζ and for each measured body mass M, gains and costs were assessed and averaged across replicates. The simulated gain surplus slope was measured across $\log(g_S)$ and $\log(M)$ for larger herbivores and evaluated as a function of both environmental richness μ and for the different categories of herbivore fermentation (see app. S2).

We found that in resource-plentiful environments, the scaling of g_S was equivalent to gut capacity scaling as $M \to \infty$. For the mass range explored here, g_S showed a slightly steeper relationship with body mass compared with gut capacity, where at the low end $\gamma \approx 0.9$ for cecum fermenters and at the high end $\gamma \approx 0.95$ for colon fermenters (app. S2). Because herbivore gut capacities scale sublinearly with body mass, it is notable that the gain surplus in these environments remained sublinear and not superlinear as one would expect from the observed mass-fat relationship.

Encounter rate constrains gains in poor environments. As resource availability declines, foragers must travel farther for each bite and are limited by the amount of food encountered during the length of the foraging bout rather than their gut capacity. In this case, the gain term is bout limited and more complex but can be estimated as $g^{\text{bout}} \approx \delta\beta n_e$, where n_e is the expected number of bites within the bout time t_{b}. In our minimal foraging model, time is accrued during two activities within the foraging bout: the expected travel time t_{t} and chewing time t_{c} associated with each bite. As such, $n_e \approx t_{\text{b}}(\mathbb{E}\{t_{\text{t}}\} + t_{\text{c}})^{-1}$ where, as previously noted, $\mathbb{E}\{t_{\text{t}}\} = \mathbb{E}\{D\}v^{-1}$, with v as the forager's velocity. Importantly, because $\mathbb{E}\{t_{\text{t}}\}$ is an expectation, we do not expect the calculation of n_e to be universally accurate because of Jensen's inequality (Denny 2017) and must instead treat this as an approximation while relying on simulation results. Because distance variance is of the same order as the distance mean, approximations such as the delta method (Hilborn and Mangel 1997) are unavailable.

With the decline in environmental richness, travel time increases across the board (app. S2). Full calculation of the gain term resulted in a solution that cannot be easily expressed, with the slope decreasing at large

body masses (fig. 3*A*, dashed blue line). Calculation of the cost term revealed a shallower slope, with similarly complex behavior in the large size class (fig. 3*A*, dashed red line). However, our simulation results revealed that the gain and cost terms were both well represented by mass allometries with single exponents, where $g^{\text{bout}} = g_0 M^{g_1}$ and $c^{\text{bout}} = c_0 M^{c_1}$.

In resource-limited environments, it is clear that the gain term has a steeper slope than the cost term such that $g_1 > c_1$. Here, the costs $c^{\text{bout}} \propto M^{0.78}$, whereas $g^{\text{bout}} \propto M^{0.93}$. From these relationships for gains and costs, we calculate the effective slope γ of the gain surplus $g_S = g^{\text{bout}} - c^{\text{bout}}$ as

$$\gamma = g_1 + \frac{(c_1 - g_1)c_0 M^{c_1}}{c_0 M^{c_1} - g_0 M^{g_1}}. \tag{3}$$

There are two behaviors of these gain and cost relationships that are important for mass-fat scaling. First, it is clear that when the gain and cost functions intersect, the denominator of equation (3) goes to zero, and $\gamma \to \infty$. For body masses near but above this point, the slope of the gain surplus achieves superlinearity. Second, the body size defining this intersection increases as the richness of the environment, μ, decreases. So as the density of available foods declines, so do gains, leaving only larger species—with greater gain surpluses—to replace daily costs and achieve $g_S > 0$.

Both simulation results and analytical approximations revealed that larger species have an advantage in resource-limited environments given their ability to consume a larger energetic surplus relative to costs despite not having reached gut capacity. This is due to a number of intersecting relationships: larger species generally have longer foraging bouts (Owen-Smith 1988), and although travel times between bites are somewhat greater for larger species (app. S2) their larger per-bite energetic yield promotes volumetric intake of forage overall. As the threshold condition, $g^{\text{bout}} = c^{\text{bout}}$, moves to higher masses with increasing resource scarcity (lower μ), the gain surplus for larger species takes on an elevated and superlinear effective slope. In this resource-limited regime, γ for herbivores of all gut types converges to the same curve, rising above unity for $\mu \lesssim 10^{-2.86}$ (fig. 4).

Spatial partitioning of resources. Resources that become more uniform with increased body size ($\zeta < 2$; app. S2) have less relative variability between encounters, ensuring that larger species have an inherent advantage in resource procurement. This mechanism has been posited as a potential driver of the evolutionary increase in body size observed among grazing mammals following the expansion of C_4 grassland ecosystems (Bhat et al. 2020). By increasing access to more uniform foods, herbivores reduce the uncertainty associated with patchier resources while elevating the probability that gains can recoup costs, though the immediate consequences of resource patchiness are size dependent.

Standardizing gains relative to costs clarifies how the scaling of resource patchiness impacts foragers across different size classes, which we define as the reserve ratio $\phi = g/c$. In our framework, $\zeta < 2$ means that the reserve ratio has a roughly constant scaling exponent of ~0.15 such that $\phi = 1.5$ for gazelle-sized herbivores ($M = 50$ kg) and

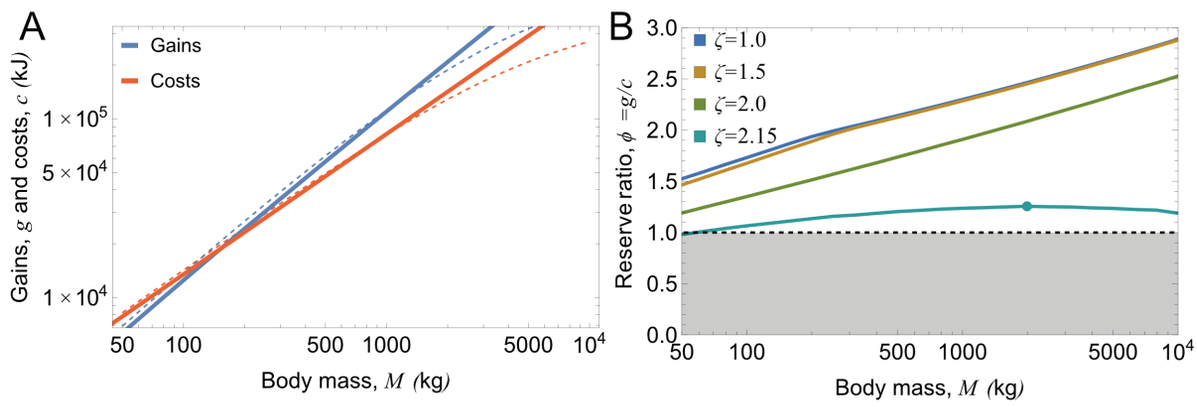


Figure 3: *A*, Daily gains (blue lines) and costs (red lines) versus forager body mass M in resource-limited environments under assumptions of $\mu = 10^{-2.8}$, $\alpha = 4$, $\zeta = 1$. Solid lines indicate daily gains and costs; dashed lines indicate analytical approximations and show increasingly poor fit as body size increases. *B*, Reserve ratio $\phi = g/c$ for different levels of patchiness ζ as function of forager body mass M. Low ζ means that experienced resource distributions become more homogeneous with increasing body size; intermediate $\zeta = 2$ means that experienced patchiness is constant across body size; high $\zeta > 2$ means that experienced patchiness increases with body size. The circle for $\zeta = 2.15$ denotes the intermediate body size at which ϕ is maximized.

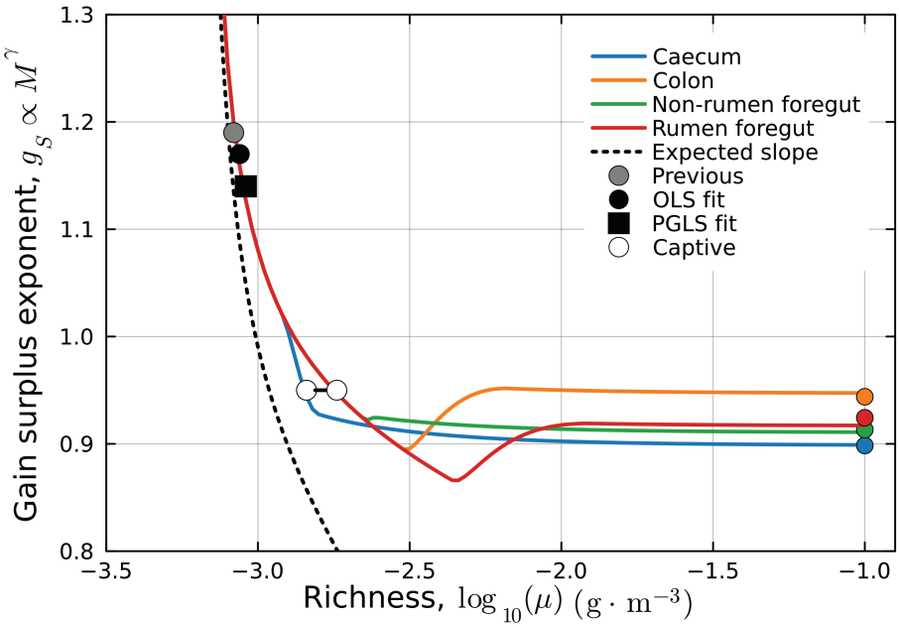


Figure 4: Daily gain surplus exponent γ as function of environmental richness μ for cecum, colon, nonrumen foregut, and rumen foregut foragers, derived from simulations (500 replicates). Analytical approximation of γ is shown for resource-limited conditions where herbivores are bout limited (dashed line) and for enriched conditions where herbivores are gut limited (colored circles). Also shown are the mass-fat scaling relationships reported here (f_1^{OLS} [black circle] and f_1^{PGLS} [black square]), as previously reported by Lindstedt and Boyce (1985), Calder (1996), and Lindstedt and Schaeffer (2002; gray circles), and for captive mammals collected by Navarrete et al. (2011; white circles).

increases to $\phi \approx 3.0$ for elephant-sized herbivores (fig. 3*B*, blue and orange lines). For resources that retain a patchy distribution, irrespective of body size ($\zeta = 2$), ϕ drops systematically given that clustering increases the mean distance between resources (fig. 3*B*, green line). If resource patchiness increases with body mass ($\zeta > 2$), as might be expected in highly engineered landscapes or when large species must travel between food islands, we observe ϕ to increase more slowly with body mass, reaching a maximum at intermediate size class (at approximately $M =$ 2,000 kg for $\zeta = 2.15$) before declining (fig. 3*B*, teal line; app. S4).

Superlinear mass-fat scaling ensures that larger species have an inherent advantage in weathering gaps in resource availability given their greater resistance to starvation. This advantage is maintained across different resource types: from resources that become more uniformly distributed with size (e.g., leaves in forests or grass in tall grass prairies) to those that retain their patchiness (masting fruits, high-quality browse). This aligns with prior work showing that foragers with larger perceptual scales—a reasonable proxy for larger body size—gain most when resources are aggregated into a few large patches, whereas fine-scale foragers optimize intake when resources are evenly distributed and patch size is uniformly small (Ritchie 1998). Yet the advantage of large size erodes if foragers themselves intensify patchiness. Along similar lines, moderate grazing pressure has been shown to create self-similar food island mosaics through a slowdown-and-aggregate feedback between consumers and vegetation (Ge and Liu 2022). In such cases, the very feedbacks that build spatial heterogeneity may undo the energetic advantages of large body size, promoting instead intermediate size classes where we observe the reserve ratio to be maximized (fig. 3*B*, teal line).

Empirical intake and fat in captivity. Our prediction of a steeper daily gain exponent relative to that of costs is a requirement for superlinear mass-fat scaling emerging from resource limitation. Seemingly in contrast, Clauss et al. (2007) and later Müller et al. (2013) compiled multiple datasets showing that dry matter intake $\propto M^{0.75}$ (though in the latter case, the authors note that intake may be steeper for larger mammals). Whereas the methods by which these data originate are numerous, they are in nearly all cases from controlled experiments in captive settings (as it would be nearly impossible to measure intake accurately in the wild). As such, the food intake and resultant fat storage would not be expected to reflect resource limitation per se, and the extent to which this information would be useful in deriving the mass-fat relationship based on the arguments we have presented is likely minimal.

In sharp contrast, the steeper gain relationship that we have derived is entirely the result of the intersection of the assumed foraging dynamics with resource scarcity. Perhaps compellingly, we note that when resource availability is elevated (higher μ), the scaling of the gain term drops from $g_1 = 0.94$ to 0.86, approaching the lower values associated with intake exponents measured in controlled settings.

Our minimal foraging model predicts that a range of mass-fat scaling relationships is expected for herbivores experiencing different degrees of resource limitation. For herbivores in resource-limited environments, the mass-fat relationship should scale superlinearly; for those in enriched environments, we would expect the scaling to be lower, approaching gut capacity as intake saturates. There is limited opportunity to examine this prediction directly, though comparison of captive versus wild mammals offers one such option. The detailed tissue measurements performed by Navarrete et al. (2011) offer insight into mass-fat scaling (Antoł and Kozłowski 2020; Wilkinson et al. 2025) among captive versus wild mammals, though they are limited to smaller species biased toward rodents, primates, and carnivores (the largest being a captive tiger at ~75 kg), with larger size classes primarily captive and smaller size classes primarily wild. Despite these potential biases, we observed the best-fit mass-fat exponent of wild species in this dataset to be 1.05 ± 0.06 and that of captive species to be 0.96 ± 0.07. Though a pairwise Wald test showed that their difference is not significant ($t_{93} = 1.01$, $P = .31$), the qualitative difference in wild versus captive mass-fat exponents accords with model predictions, where captive animals with ready access to resources evince a shallower mass-fat relationship.

Populations on the Edge

The superlinear scaling of gain surplus with body size—and, by proxy, the mass-fat relationship—is inevitable if (1) gains have a steeper body mass scaling than that of costs and (2) the environment is resource limited such that species operate relatively close to the margin (close to the intersection of gains and costs). Our minimal model captures specific mechanisms underlying the foraging process (fig. 1); however, the emergence of superlinear mass-fat scaling from forage surplus is not bound by the constraints of this particular representation. Yet the stated preconditions of this general superlinear scaling rule raise the following question: how close to the margin do individual herbivores need to operate to express the observed scaling of γ?

We calculated the surplus required to achieve the observed mass-fat scaling, investigating to what extent this informs our understanding of resource limitation in natural environments. By setting $\gamma^* \equiv f_1^{\text{PGLS,OLS}}$ in equation (3), we solved for the reserve ratio ϕ, where

$$\phi\Big|_{\gamma=\gamma^*} = \frac{g^{\text{bout}}}{c^{\text{bout}}}\Big|_{\gamma=\gamma^*} = 1 - \frac{c_1 - g_1}{\gamma^* - g_1}. \tag{4}$$

Here, ϕ represents the relative gain driving the observed mass-fat scaling, which immediately communicates two important messages: the reserves required (1) depend on only the exponents of gains and costs and (2) are independent of body mass. The relationship in equation (4) has some limitations. First, it is relevant only in resource-limited environments, where herbivores do not accrue enough gain to fill their gut. Second, the slopes of the gain and cost terms are specific to the resource environment giving rise to the observed mass-fat scaling, where $g_1 \approx 0.93$ and $c_1 \approx 0.78$ for environments where patchiness scaling $\zeta \leq 2$.

Combining the (g_1, c_1) values with the empirical mass-fat scaling, we obtained $\phi = 1.61$ (OLS) and 1.69 (PGLS), suggesting that herbivores obtaining 61%–69% more energetic gain relative to costs will produce the observed mass-fat superlinear scaling relationship. However, in a stable population operating at or near carrying capacity, daily foraging gains are not only used to account for daily costs but also must, on average, account for the additional costs associated with ontogenetic growth and reproduction. To estimate the minimal demographic costs that must be subtracted from the surplus available for fat storage, we used the mass balance framework defined by West et al. (2001), presented as $B_0 m^{3/4} = E_m \dot{m} + B_m m$, where m is the mass of a growing animal and E_m and B_m represent the energetic costs of tissue synthesis and maintenance, respectively. We calculate daily demographic costs as

$$\kappa = \frac{E_m(\epsilon_A M - m_0)}{t_\ell} + \frac{2E_m\epsilon_J M}{t_\ell}, \tag{5}$$

where $\epsilon_A = 0.99$ specifies the proportion of a species' asymptotic mass M defining the adult size class, $\epsilon_J = 0.75$ is the assumed proportion of asymptotic mass defining the end of a juvenile's reliance on parental care, m_0 is size at birth, and t_ℓ is expected lifetime in days. The first term in equation (5) is thus the per-diem lifetime energetic cost associated with an individual growing to its adult mass, whereas the second term is the per-diem energetic cost of supporting two offspring (i.e., replacement) from embryogenesis to size $\epsilon_J M$.

Applying mammalian scaling relationships to equation (5) (see app. S2), we found that $\kappa = \kappa_0 M^{0.75}$. We account for daily demographic costs in our reserve ratio as

$$\phi^{\text{dem}}\big|_{\gamma=\gamma^*} = \left.\frac{g^{\text{bout}} - \kappa}{c^{\text{bout}}}\right|_{\gamma=\gamma^*} = 1 - \frac{c_1 - g_1}{\gamma^* - g_1} - \frac{\kappa_0}{c_0}, \quad (6)$$

where $\kappa_0/c_0 \approx 0.24$ in the regime where we attained the observed mass-fat scaling. Together, $\phi^{\text{dem}} \approx 1.37$ (OLS) to 1.45 (PGLS), meaning that if herbivores—regardless of body size—reach a 37%–45% forage surplus, they are expected to meet the minimum conditions required to both achieve population-level stability and attain the observed mass-fat scaling relationship. It is important to note that this surplus value is an upper bound, or ceiling, based on the averaged demographic costs of growth and reproduction. With the additional costs of more than two offspring and the energetic resynthesis costs of lost fat reserves following bouts of starvation (Yeakel et al. 2018) among other costs, the per-diem demographic load (eq. [5]) will increase, reducing the realized value of ϕ^{dem}.

This surplus is sensitive to resource patchiness in addition to the scaling of gains and costs accrued by the forager (fig. 5*A*). The scaling of resource patchiness (ζ) alters the mean and variability of the distances separating a forager's bites, which in turn alters the energetic gains and costs within foraging bouts. As patchiness increases (causing an increase in both the mean and the variability of bite distances), the exponents associated with gains and costs decline, which reduces the ϕ^{dem} ceiling (fig. 3*B*). The elements governing bite distances determine the energetic edge (where gains balance costs) and the distance from it required to express the observed fat scaling. The demography-adjusted reserve ratio ϕ^{dem} quantifies this distance, whereas density-dependent feedbacks are expected to depress the effective resource availability, pushing populations toward the edge and steepening the slope. We therefore read the empirical mass-fat exponent as a signal of how tightly scarcity drives systems to that acquisition-limited edge.

Importantly, the demography-adjusted reserve ratio is fully general and independent of foraging models, requiring only that gains and costs follow single-term power law relationships and that gains are steeper than costs. After paying both metabolic and demographic costs, individuals must still accumulate a surplus equal to a fixed fraction of their total daily metabolic expenditure to accumulate fat fast enough to achieve the observed mass-fat scaling. If the mass-fat exponent is unconstrained to the empirical value, our framework predicts that populations operating within a slimmer margin (lower ϕ) will exhibit a steeper mass-fat slope (fig. 5*B*). Well-provisioned populations on the other hand—such as those in captivity—will show a more shallow relationship converging on gut capacity limits.

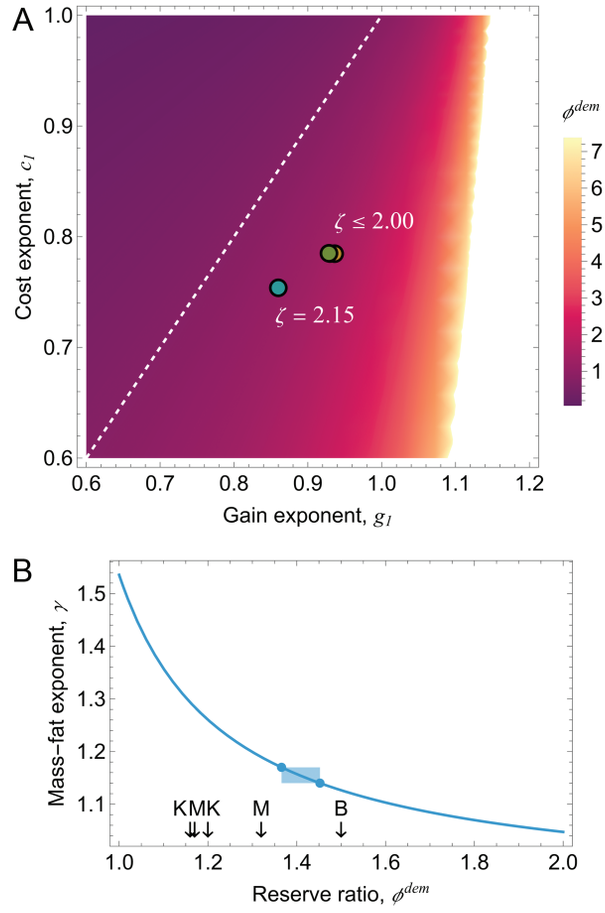


Figure 5: *A*, Demographic reserve ratio required to maintain observed empirical mass-fat scaling relationship, $\phi^{\text{dem}}|_{\gamma=\gamma^*}$, as function of gain exponent g_1 and cost exponent c_1. This ratio accounts for the minimum demographic requirements to grow to adult body mass and to maintain a population at carrying capacity (shown here from the OLS fit). Colored circles denote ϕ^{dem} values for gain/cost scaling relationships emerging from patchiness exponents: $\zeta \le 2$ (nearly overlapping; $\phi^{\text{dem}} \approx 1.37$) and $\zeta = 2.15$ ($\phi^{\text{dem}} = 1.02$). The dashed line denotes where $g_1 = c_1$. *B*, Unconstrained gain surplus exponent γ as function of reserve ratio (with gain and cost exponents set as in *A* for $\zeta = 1$). The shaded region shows the $\phi^{\text{dem}} = 1.37$ to 1.45 reserve ratio predicted from the observed mass-fat exponents. Arrows with letters denote empirical measures of surplus for three ungulate species during periods of fat accumulation: K = kudu (Owen-Smith 1997); M = moose (Renecker and Hudson 1989); B = black-tailed deer (Parker et al. 1999).

Because energetic gains in natural settings are difficult to measure, there are few opportunities to verify our analytical ϕ^{dem} against field observations. Some notable exceptions include estimated intake relative to expenditure for black-tailed deer (Channel Island, Alaska; Parker et al. 1999), semiwild moose (central Alberta; Renecker and Hudson 1989), and semiwild kudu (northern South

Africa; Owen-Smith 1997; arrows with letters in fig. 5*B*). Both black-tailed deer and moose inhabit environments with severe winters, where fat stores are accumulated during the spring/summer. Although seasonal fluxes are less intense for kudu, they must similarly accumulate stores during the wet growing seasons. As we demonstrate in appendix S3, mass-fat scaling is expected to match the scaling of daily gain surplus during periods of fat accumulation rather than expenditure. During these periods of accumulation, black-tailed deer exceed their energetic demand by ~50% and moose by ~32% during spring, declining to ~17% by late autumn. Kudu exceed their requirements by ~20% in the midwet season, declining to ~16% by the early dry season. This lower value for kudu aligns with more limited fat stores observed among African ungulates, which may be associated with heat tolerance and/or predator avoidance (Owen-Smith 1997). Together, these observations—particularly for species in environments where significant fat storage determines survival—straddle our calculation of ϕ^{dem}, where the expected ceiling for surplus is 37%–45%. This alignment supports the notion that the observed superlinear mass-fat scaling originates from animals saving where they can while living on the edge.

Beyond Contemporary Terrestrial Herbivory

We show that across terrestrially, aquatically, and even aerially foraging mammals, the superlinear mass-fat scaling remains remarkably consistent (fig. 2). That the inclusion of multiple extremely large-bodied mysticete and odontocete taxa fall within the observed relationship is telling. Free from gravitational limitations, one may suppose that marine mammals would evince a mass-fat relationship that is apart from that observed for their terrestrial counterparts; however, their exponents are statistically indistinguishable. Yet if we instead follow the argument proposed here—that the limitations of fat accumulation arise from constraints induced by the mechanics of foraging and resource scarcity—one might expect terrestrial and aquatic mass-fat scaling relationships to be aligned.

Our specific model focuses on evaluating herbivory within a vegetative resource volume; however, it is general in scope, and few adjustments would be needed to capture different foraging environments or alternative trophic levels. For example, revising the model for mysticete filter feeders would require altering resource energy density (Goldbogen et al. 2011), bite size scaling (Goldbogen et al. 2010; Kahane-Rapport and Goldbogen 2018), the metabolic costs associated with lunge feeding (Goldbogen et al. 2008, 2012), and the scaling of velocity and reaction cross sections (Cronin et al. 2017), much of which has been measured.

We expect these alternate maritime parameterizations to impact scaling intercepts rather than exponents such that the relative daily gain versus cost relationship will not be markedly different than those estimated for terrestrial species, though this deserves a thorough investigation. For example, the volumetric scaling of a mysticete bite, measured as the mass of seawater engulfment $M_w \propto M^{1.0}$ (Goldbogen et al. 2010), does not stray far from the bite size scaling of terrestrial herbivores ($\beta \propto M^{0.96}$; Shipley et al. 1994). Alternatively, the notion that metabolic costs may scale more shallowly with large marine taxa, as has been proposed on the basis of the observed enlargement—and potentially lower metabolic rate—of adipocyte cells (Pereira and Ribeiro 2022), would further serve to support the origin of superlinear mass-fat scaling described here. Among nonmammalian marine species, we note that the scaling of liver weight with body mass for lamniformes (specifically white sharks) is also superlinear (Lingham-Soliar 2005). Liver serves as the primary energy storage tissue for sharks, and that liver mass evinces a superlinear exponent on par with mammalian fat mass is perhaps compelling.

A potentially useful application of our framework is to turn the problem on its head to investigate extinct species. For example, the mechanics of foraging for sauropod dinosaurs may be represented by minor changes to our foraging model. Long sauropod necks enable atypically large reaction cross sections (Clauss and Hummel 2005), sometimes referred to as feeding envelopes (Sander et al. 2011), whereas the allometry of bite size can be estimated from morphometrics (Hummel and Clauss 2011). Although metabolic costs are likely rough estimates (Sander and Clauss 2008), it would appear within reach to leverage similar ecological models to explore whether a superlinear mass-fat scaling is realistic for such enormously large terrestrial herbivores, potentially allowing one to address whether some dinosaurs were fat and, if so, how fat were they?

Conclusions

Mammals use fat in a variety of ways, from insulation, buoyancy, and cognition to maintaining energetic reserves for use in times of scarcity. The adipose tissue from which these reserves are composed famously scales superlinearly with body mass, with a previously measured exponent of $f_1 = 1.19$ (Calder 1996), though its origin has been a mystery. Here we have both reevaluated and added to the original mass-fat relationship, confirming its superlinearity ($f_1 = 1.14$ to 1.17 on the basis of PGLS and OLS fits, respectively), despite recent investigations suggesting isometry (cf. Antoł and Kozłowski 2020). We make the case that the origin of the mass-fat scaling can be explained by the mechanics of foraging within a resource-limited environment, where a 37%–45% surplus,

regardless of size, is expected to produce the observed relationship.

Although much can be gleaned from the energetics of daily foraging processes, it is the coupled nature of daily dynamics—in environments that fluctuate on different scales—that impacts the selective landscape. Exploring how energetic stores contribute to the success or failure of species of different sizes occupying different positions in food webs is clearly needed to understand how these physiological limitations shape long-term macroevolutionary processes.

Acknowledgments

We thank Uttam Bhat, Luke Fannin, Matthew Hutchinson, Pedro Ugarte, Nathaniel J. Dominy, and two anonymous referees for insightful discussions and comments that contributed to and greatly improved the quality of this manuscript. This project was supported by the National Science Foundation (DMS-2424994 to J.D.Y. and S.K.; DMS-2424995 to G.B.; ABI-1759846 to E.J.M.), the Conard Initiative on the Foundations of Complexity in Nature and Society (to L.M.A.B.), and travel support from the Santa Fe Institute (to J.D.Y.).

Statement of Authorship

J.D.Y., C.P.K., and L.M.A.B. conceived the analysis; J.D.Y., M.F., and E.J.M. performed data curation and empirical analyses; J.D.Y. and A.C.A. developed and analyzed the theoretical model; J.D.Y., M.F., S.K., and G.A.B. interpreted the results; J.D.Y., C.P.K., and L.M.A.B. conducted and interpreted supplemental analyses; all authors wrote the original draft and contributed to review and editing.

Data and Code Availability

Code and data are available on Zenodo (https://doi.org/10.5281/zenodo.17280284; Yeakel 2026).

Literature Cited

Antoł, A., and J. Kozłowski. 2020. Scaling of organ masses in mammals and birds: phylogenetic signal and implications for metabolic rate scaling. ZooKeys 982:149.

Bergman, C. M., J. M. Fryxell, C. C. Gates, and D. Fortin. 2001. Ungulate foraging strategies: energy maximizing or time minimizing? Journal of Animal Ecology 70:289–300.

Bhat, U., C. P. Kempes, and J. D. Yeakel. 2020. Scaling the risk landscape drives optimal life-history strategies and the evolution of grazing. Proceedings of the National Academy of Sciences of the USA 117:1580–1586.

Brodin, A. 2010. The history of scatter hoarding studies. Philosophical Transactions of the Royal Society B 365:869–881.

Calder, W. A., III. 1996. Size, function, and life history. Courier, Chelmsford, MA.

Carbone, C., D. Codron, C. Scofield, M. Clauss, and J. Bielby. 2014. Geometric factors influencing the diet of vertebrate predators in marine and terrestrial environments. Ecology letters 17:1553–1559.

Chusyd, D. E., T. R. Nagy, L. Golzarri-Arroyo, S. L. Dickinson, J. R. Speakman, C. Hambly, M. S. Johnson, D. B. Allison, and J. L. Brown. 2021. Adiposity, reproductive and metabolic health, and activity levels in zoo Asian elephant (*Elephas maximus*). Journal of Experimental Biology 224:jeb219543.

Clauss, M., and J. Hummel. 2005. The digestive performance of mammalian herbivores: why big may not be that much better. Mammal Review 35:174–187.

Clauss, M., A. Schwarm, S. Ortmann, W. J. Streich, and J. Hummel. 2007. A case of non-scaling in mammalian physiology? body size, digestive capacity, food intake, and ingesta passage in mammalian herbivores. Comparative Biochemistry and Physiology A 148:249–265.

Coverdale, T. C., T. R. Kartzinel, K. L. Grabowski, R. K. Shriver, A. A. Hassan, J. R. Goheen, T. M. Palmer, and R. M. Pringle. 2016. Elephants in the understory: opposing direct and indirect effects of consumption and ecosystem engineering by megaherbivores. Ecology 97:3219–3230.

Cronin, T. W., J. I. Fasick, L. E. Schweikert, S. Johnsen, L. J. Kezmoh, and M. F. Baumgartner. 2017. Coping with copepods: do right whales (*Eubalaena glacialis*) forage visually in dark waters? Philosophical Transactions of the Royal Society B 372:20160067.

Denny, M. 2017. The fallacy of the average: on the ubiquity, utility and continuing novelty of Jensen's inequality. Journal of Experimental Biology 220:139–146.

Fryxell, J. M. 1991. Forage quality and aggregation by large herbivores. American Naturalist 138:478–498.

Ge, Z., and Q.-X. Liu. 2022. Foraging behaviours lead to spatiotemporal self-similar dynamics in grazing ecosystems. Ecology Letters 25:378–390.

George, J. C., J. R. Bockstoce, A. E. Punt, and D. B. Botkin. 2007. Preliminary estimates of bowhead whale body mass and length from Yankee commercial oil yield records. Center for the Study of the Environment 98105:5020.

Goldbogen, J. A., J. Calambokidis, D. A. Croll, J. T. Harvey, K. M. Newton, E. M. Oleson, G. Schorr, and R. E. Shadwick. 2008. Foraging behavior of humpback whales: kinematic and respiratory patterns suggest a high cost for a lunge. Journal of Experimental Biology 211:3712–3719.

Goldbogen, J. A., J. Calambokidis, D. A. Croll, M. F. McKenna, E. Oleson, J. Potvin, N. D. Pyenson, G. Schorr, R. E. Shadwick, and B. R. Tershy. 2012. Scaling of lunge-feeding performance in rorqual whales: mass-specific energy expenditure increases with body size and progressively limits diving capacity. Functional Ecology 26:216–226.

Goldbogen, J. A., J. Calambokidis, E. Oleson, J. Potvin, N. D. Pyenson, G. Schorr, and R. Shadwick. 2011. Mechanics, hydrodynamics and energetics of blue whale lunge feeding: efficiency dependence on krill density. Journal of Experimental Biology 214:131–146.

Goldbogen, J. A., J. Potvin, and R. E. Shadwick. 2010. Skull and buccal cavity allometry increase mass-specific engulfment capacity in fin whales. Proceedings of the Royal Society B 277:861–868.

Hilborn, R., and M. Mangel. 1997. The ecological detective: confronting models with data. Monographs in Population Biology. Princeton University Press, Princeton, NJ.

Holland, E., J. Aegerter, and C. Dytham. 2009. Comparing resource representations and choosing scale in heterogeneous landscapes. Landscape Ecology 24:213–227.

Hou, C., W. Zuo, M. E. Moses, W. H. Woodruff, J. H. Brown, and G. B. West. 2008. Energy uptake and allocation during ontogeny. Science 322:736–739.

Hummel, J., and M. Clauss. 2011. Sauropod feeding and digestive physiology. Pages 11–33 *in* N. Klein, K. Remes, C. T. Gee, and P. M. Sander, eds. Biology of the sauropod dinosaurs: understanding the life of giants. Indiana University Press, Bloomington.

Kahane-Rapport, S. R., and J. A. Goldbogen. 2018. Allometric scaling of morphology and engulfment capacity in rorqual whales. Journal of Morphology 279:1256–1268.

Kartzinel, T. R., J. R. Goheen, G. K. Charles, E. DeFranco, J. E. Maclean, T. O. Otieno, T. M. Palmer, and R. M. Pringle. 2014. Plant and small-mammal responses to large-herbivore exclusion in an African savanna: five years of the UHURU experiment. Ecology 95:787–787.

Kelt, D. A. 2011. Comparative ecology of desert small mammals: a selective review of the past 30 years. Journal of Mammalogy 92:1158–1178.

Kohi, E. M., W. F. de Boer, M. J. Peel, R. Slotow, C. van der Waal, I. M. Heitkönig, A. Skidmore, and H. H. Prins. 2011. African elephants *Loxodonta africana* amplify browse heterogeneity in African savanna. Biotropica 43:711–721.

Kramer, K., and H. Prins. 2010. Allometric scaling of resource acquisition by ruminants in dynamic and heterogeneous environments. Ecological Modelling 221:2555–2564.

Lindstedt, S. L., and M. S. Boyce. 1985. Seasonality, fasting endurance, and body size in mammals. American Naturalist 125:873–878.

Lindstedt, S. L., and W. A. Calder III. 1981. Body size, physiological time, and longevity of homeothermic animals. Quarterly Review of Biology 56:1–16.

Lindstedt, S. L., and P. J. Schaeffer. 2002. Use of allometry in predicting anatomical and physiological parameters of mammals. Laboratory Animals 36:1–19.

Lingham-Soliar, T. 2005. Caudal fin allometry in the white shark *Carcharodon carcharias*: implications for locomotory performance and ecology. Naturwissenschaften 92:231–236.

Lund, J., T. Smith, D. Chatwin, W. Sanger, J. T. duPasquier, and A. Kirkpatrick. 2025. American offshore whaling database. https://whalinghistory.org/av/.

McTavish, E. J. 2025. Chronosynth: match dates from chronograms to synthetic-tree nodes. https://github.com/OpenTreeOfLife/chronosynth.

Michonneau, F., J. W. Brown, and D. J. Winter. 2016. rotl: an R package to interact with the Open Tree of Life data. Methods in Ecology and Evolution 7:1476–1481.

Millar, J., and G. Hickling. 1990. Fasting endurance and the evolution of mammalian body size. Functional Ecology 4:5–12.

Müller, D. W., D. Codron, C. Meloro, A. Munn, A. Schwarm, J. Hummel, and M. Clauss. 2013. Assessing the Jarman–Bell principle: scaling of intake, digestibility, retention time and gut fill with body mass in mammalian herbivores. Comparative Biochemistry and Physiology A 164:129–140.

Nagy, K. A. 2005. Field metabolic rate and body size. Journal of Experimental Biology 208:1621–1625.

Navarrete, A., C. P. Van Schaik, and K. Isler. 2011. Energetics and the evolution of human brain size. Nature 480:91–93.

Owen-Smith, N. 1997. Control of energy balance by a wild ungulate, the kudu (*Tragelaphus strepsiceros*) through adaptive foraging behaviour. Proceedings of the Nutrition Society 56:15–24.

Owen-Smith, R. N. 1988. Megaherbivores: the influence of very large body size on ecology. Cambridge University Press, Cambridge, MA.

Parker, K. L., M. P. Gillingham, T. A. Hanley, and C. T. Robbins. 1999. Energy and protein balance of free-ranging black-tailed deer in a natural forest environment. Wildlife Monographs 143:3–48.

Pereira, W. R. L. S., and F. L. Ribeiro. 2022. The metabolic origins of big size in aquatic mammals. https://doi.org/10.48550/arXiv.2210.02183.

Pitts, G. C., and T. R. Bullard. 1968. Some interspecific aspects of body composition in mammals. Pages 45–70 *in* N. R. Council, ed. Body composition in animals and man. National Academy of Sciences, Washington, DC.

Pond, C. M. 1992. An evolutionary and functional view of mammalian adipose tissue. Proceedings of the Nutrition Society 51:367–377.

Pond, C. M., and C. A. Mattacks. 1985. Body mass and natural diet as determinants of the number and volume of adipocytes in eutherian mammals. Journal of Morphology 185:183–193.

Rallings, T., C. P. Kempes, and J. D. Yeakel. 2024. On the dynamics of mortality and the ephemeral nature of mammalian megafauna. American Naturalist 204:274–288.

Renecker, L. A., and R. J. Hudson. 1989. Ecological metabolism of moose in aspen-dominated boreal forests, central Alberta. Canadian Journal of Zoology 67:1923–1928.

Ritchie, M. E. 1998. Scale-dependent foraging and patch choice in fractal environments. Evolutionary Ecology 12:309–330.

Roff, D. A. 2002. Life history evolution. Sinauer, Sunderland, MA.

Ryg, M., C. Lydersen, L. Knutsen, A. Bjørge, T. Smith, and N. Øritsland. 1993. Scaling of insulation in seals and whales. Journal of Zoology 230:193–206.

Sander, P. M., A. Christian, M. Clauss, R. Fechner, C. T. Gee, E.-M. Griebeler, H.-C. Gunga, et al. 2011. Biology of the sauropod dinosaurs: the evolution of gigantism. Biological Reviews 86:117–155.

Sander, P. M., and M. Clauss. 2008. Sauropod gigantism. Science 322:200–201.

Schook, M. W., D. E. Wildt, M. A. Raghanti, B. A. Wolfe, and P. M. Dennis. 2015. Increased inflammation and decreased insulin sensitivity indicate metabolic disturbances in zoo-managed compared to free-ranging black rhinoceros (*Diceros bicornis*). General and Comparative Endocrinology 217:10–19.

Shipley, L. A., J. E. Gross, D. E. Spalinger, N. T. Hobbs, and B. A. Wunder. 1994. The scaling of intake rate in mammalian herbivores. American Naturalist 143:1055–1082.

Voigt, C. C., K. Sörgel, and D. K. Dechmann. 2010. Refueling while flying: foraging bats combust food rapidly and directly to power flight. Ecology 91:2908–2917.

Weil, C., F. Lefèvre, and J. Bugeon. 2013. Characteristics and metabolism of different adipose tissues in fish. Reviews in Fish Biology and Fisheries 23:157–173.

West, G. B., J. H. Brown, and B. J. Enquist. 2001. A general model for ontogenetic growth. Nature 413:628–631.

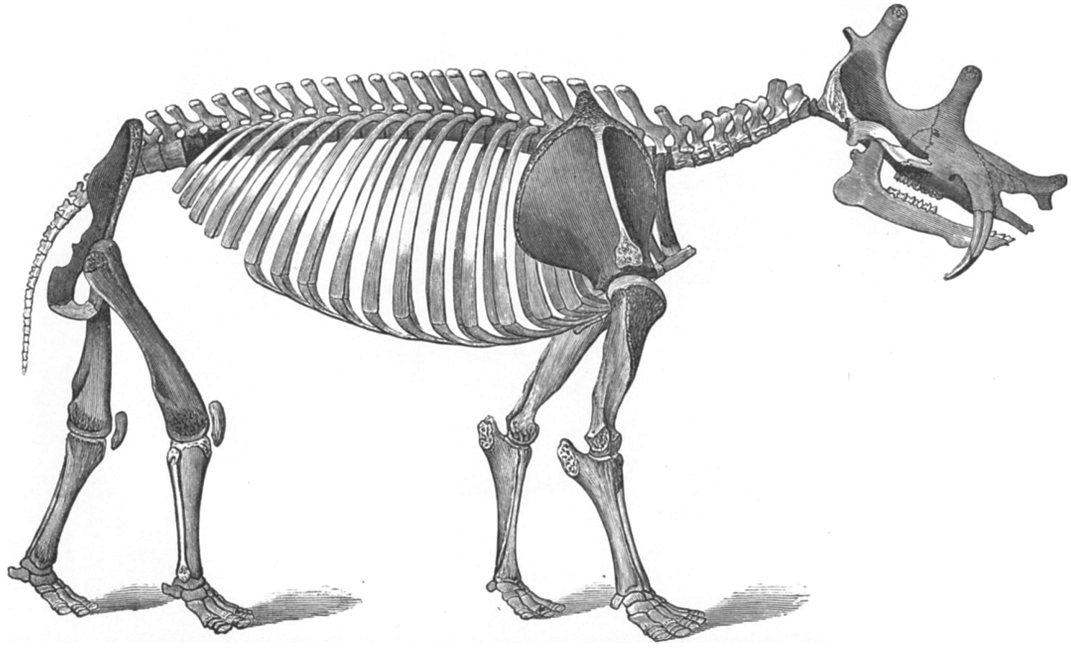
Wilkinson, C., U. Brose, A. Dyer, M. R. Hirt, and R. Ryser. 2025. A mechanistic approach to animal dispersal—quantifying energetics and maximum distances. Ecology Letters 28:e70085.

Yeakel, J. D. 2026. jdyeakel/fatscaling.jl: Fatscaling. Version 3.0. Zenodo, https://doi.org/10.5281/zenodo.20367155.
Yeakel, J. D., U. Bhat, and S. D. Newsome. 2020. Caching in or falling back at the Sevilleta: the effects of body size and seasonal uncertainty on desert rodent foraging. American Naturalist 196:241–256.
Yeakel, J. D., C. P. Kempes, and S. Redner. 2018. Dynamics of starvation and recovery predict extinction risk and both Damuth's law and Cope's rule. Nature Communications 9:1–10.
Žliobaitė, I., and M. Fortelius. 2018. Dental functional morphology predicts the scaling of chewing rate in mammals. Journal of Biomechanics 67:32–36.

References Cited Only in the Online Enhancements

Andermann, T., C. A. E. Strömberg, A. Antonelli, and D. Silvestro. 2022. The origin and evolution of open habitats in North America inferred by Bayesian deep learning models. Nature Communications 13:4833.
Damuth, J. 1987. Interspecific allometry of population density in mammals and other animals: the independence of body mass and population energy-use. Biological Journal of the Linnean Society 31:193–246.
Darling, D. A., and A. J. Siegert. 1953. The first passage problem for a continuous Markov process. Annals of Mathematical Statistics 24:624–639.
Larramendi, A. 2015. Shoulder height, body mass, and shape of proboscideans. Acta Palaeontologica Polonica 61:537–574.
Pawar, S., A. I. Dell, and V. M. Savage. 2012. Dimensionality of consumer search space drives trophic interaction strengths. Nature 486:485–489.
Pond, C. M. 1978. Morphological aspects and the ecological and mechanical consequences of fat deposition in wild vertebrates. Annual Review of Ecology and Systematics 9:519–570
Strömberg, C. A. E. 2011. Evolution of grasses and grassland ecosystems. Annual Review of Earth and Planetary Sciences 39:517–544.
Yeakel, J. D., M. C. Hutchinson, C. P. Kempes, P. L. Koch, J. L. Gill, and M. M. Pires. 2024. Bioenergetic trophic trade-offs determine mass-dependent extinction thresholds across the Cenozoic. https://doi.org/10.48550/arXiv.2410.18849 .

Associate Editor: S. K. Morgan Ernest
Data Editor: Benedicte Bachelot
Editor: Volker H. W. Rudolf



"*Loxolophodon cornutus* Cope. . . . The darkly shaded portions are those in my possession; the feet and caudal and cervical vertebræ are restored after Marsh (Uintatherium); the lower jaw after Osborn." From "The Amblypoda (Continued)" by E. D. Cope (*The American Naturalist*, 1885, 19:40–55).